Application of WBT for unbounded acoustic radiation problems with an approach for substitution of complex boundary shapes

Islam Elbahnasy, Tamas Mocsai, Petra Silar, Hans-Herwig Priebsch
Virtual Vehicle Research and Test Center, Area C NVH Friction
Inffeldgasse 21A, A-8010, Graz, Austria
e-mail: **islam.elbahnasy@v2c2.at**

Abstract

The Wave Based Technique (WBT) constitutes an upcoming simulation technique, which results in increased numerical efficiency compared to FEM and BEM approaches in solving the Helmholtz equation. The shape functions of the FEM and BEM satisfy the boundary conditions exactly, while the WBT shape functions are exact solutions of the differential equation, but not necessarily fulfill the boundary conditions. Recent developments have shown the applicability of the WBT for unbounded problems such as sound radiation and scattering. A disadvantage of the standard WBT is that the method can only handle geometrically simple problems, otherwise both the effort of the model setup and the solution of the resulted large numerical model will pose unwanted challenges. The boundary of a WB model roughly approximates the shape of the original complex boundary surface to be modeled. Therefore, when dealing with such geometrical simplifications, the boundary conditions, prescribed on a complex boundary surface (e.g. nodal velocities of a complex FE mesh), are usually mapped to the simplified WBT boundary surfaces. The final accuracy of such a geometrical approximation and mapping procedure can be hardly assessed a-priori, as it is highly problem specific. To avoid the unknown influences of such simplifications, an approach is presented, where the complex boundary data is described by the solution functions (wave functions) themselves. The complex boundary shape (of a structural FE model for example), located outside the WB boundary surfaces, is treated as a virtual boundary, whose velocity distribution is approximated by linear combinations of elementary WB solutions. The approach is presented by means of a principle test example and validated in comparison with a reference BEM solution of the same problem. Results obtained by the new approach are furthermore compared with results achieved by the standard mapping of the boundary conditions.

1 Introduction

In several engineering areas, methodologies based on the Trefftz approach [4] have received a significant recognition over the last decades. The main reason for rediscovering the Trefftz methods is based on the fact that they use the exact solutions of the governing differential equation for the field variables approximation. Especially when solving problems exhibiting a wave-like nature, such as acoustics, structural dynamics or electromagnetic problems, this becomes a major advantage in contrast to the conventional element-based methods.

The Wave Based Technique (WBT) is an alternative deterministic technique for the analysis of vibro-acoustic problems [1]. The method is based on an indirect Trefftz approach, in that the dynamic response variables are described using wave functions which exactly satisfy the governing differential equation. In this way no approximation error is made inside the domain. However, the wave functions may violate the boundary and

continuity conditions between fluid subdomains. Enforcing the residual boundary and continuity errors to zero in a weighted residual scheme yields a linear system of equations [2].

Solution of this equation system results in the contribution factors of the wave functions used in the expansion of the dynamic field variables. The WBT has been applied successfully for many steady-state structural dynamic problems, interior acoustic problems, interior vibro-acoustic problems and exterior vibro-acoustic problems. It is shown that, due to the small model size and the enhanced convergence characteristics, the WBT has a superior numerical performance as compared to the element based methods [8]. As a result, problems at higher frequencies may be tackled [5].

This paper discusses the novel approach of WBT by using of Virtual Boundary Concept (VBC). The aim of the approach is to aid the WBT to handle the complex geometrical cases without losing the advantage of low system size. The main idea is to describe the complex boundary data by the wave functions themselves. The complex boundary shape (of a structural FE model for example), located outside the WB boundary surface, is treated as a virtual boundary, whose velocity distribution is approximated by linear combinations of elementary WB solutions. The first part of this paper briefly addresses the general acoustic problem setting and the WB modeling techniques used for the acoustic radiation problem. A second part is devoted to the discussion of the novel approach Virtual Boundary Concept. Finally, the VBC is applied in complex boundary example, in order to both illustrate its potential and validate the accuracy of the obtained results.

2 Problem definition

Consider a generic unbounded acoustic radiation problem shown in figure 1. The steady-state acoustic pressure inside the problem domain is governed by the homogeneous Helmholtz equation:

$$\Delta p + k^2 p = 0, \quad r \in \Omega \tag{1}$$

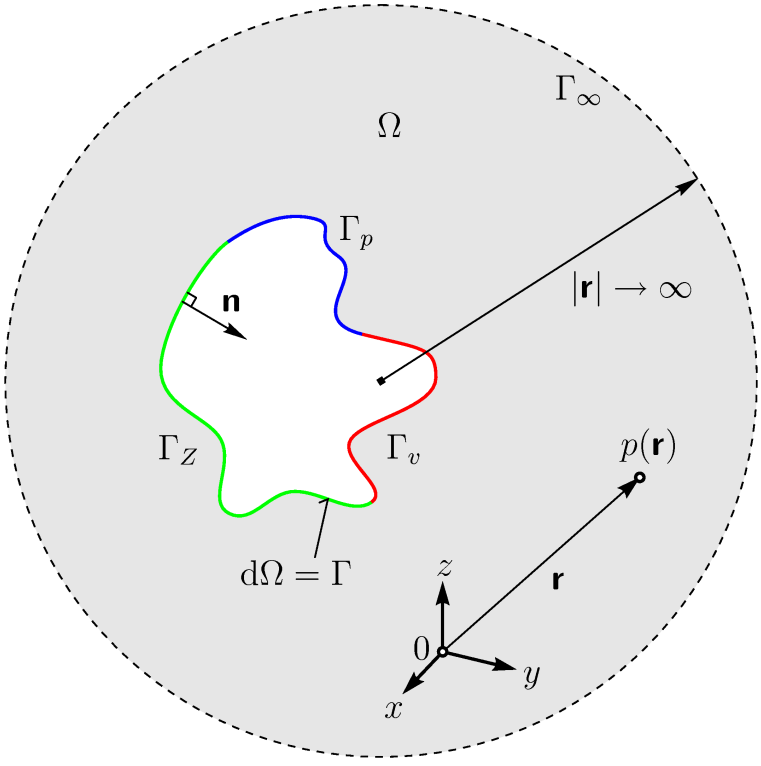

Figure 1: Unbounded acoustic radiation problem

with ω the circular frequency and $k = \omega/c$ the acoustic wave number. The acoustic fluid is characterized by the density ρ and the speed of sound c. The problem boundary Γ is consisting of 2 parts: the physical part of the boundary Γ and the boundary at infinity, Γ_∞. Based on the three types of applicable acoustic boundary conditions, the physical boundary can be further divided in three non-overlapping parts: $\Gamma = \Gamma_v \cup \Gamma_p \cup \Gamma_Z$ [2], where *v, p and Z* are, respectively, acoustic velocity, acoustic pressure and impedance. The velocity operator $\mathcal{L}_v(\bullet)$ is defined as:

$$\mathcal{L}_v = \frac{j}{\rho\omega}\frac{\partial \bullet}{\partial n}$$

the boundary condition residuals [6] can be written as:

$$r \in \Gamma_v: \quad R_v = \mathcal{L}_v(p(r)) - \bar{v}_n = 0, \tag{2a}$$

$$r \in \Gamma_p: \quad R_p = p(r) - \bar{p}(r) = 0, \tag{2b}$$

$$r \in \Gamma_Z: \quad R_Z = \mathcal{L}_v(p(r)) - \frac{p(r)}{\bar{Z}_n(r)} = 0, \tag{2c}$$

where the quantities $\bar{v}_n$, $\bar{p}$ and $\bar{Z}_n$ are, respectively, the imposed normal velocity, pressure and normal impedance. At the boundary Γ_∞ at infinity the Sommerfeld radiation condition for outgoing waves is applied. This condition ensures that no acoustic energy is reflected at infinity and is expressed as:

$$\lim_{|r|\to\infty}\left(|r|\left(\frac{\partial p(r)}{\partial |r|}\right) + jkp(r)\right) = 0. \tag{3}$$

Solution of the Helmholtz equation (1) together with the associated boundary conditions (2a)-(2c) and (3) yields a unique dynamic acoustic pressure field p(**r**).

3 Wave Based Technique for acoustic radiation problem

Various strategies were developed in order to handle the unbounded problems using the standard finite element schemes, such as non-reflecting boundary condition, infinite elements or perfectly matched layers. All these concepts, although based on different approaches, have the same basic idea in common, namely, introducing an artificial truncation boundary that divides the infinite domain into two regions - a bounded and unbounded one [7]. Similarly to those, an additional treatment of the conventional WB formulation is required to tackle problems involving unbounded domains. By introducing an artificial truncation boundary Γ_T (figure 2), the solution domain Ω is divided into a bounded and unbounded part $\Omega = \Omega^b + \Omega^u$. In the bounded part, the WB formulation for interior problems can be applied, whereas, in the unbounded part functions, which additionally satisfy the Sommerfeld radiation condition (3), are employed.

3.1 Bounded domain

For the bounded subdomain each acoustic wave function satisfies the homogenous Helmholtz equation (1). A linear combination of the shape functions approximates the exact pressure solution

$$p^b(r) \approx \hat{p}^b(r) = \sum_{i=1}^{M} p_i^b \Phi_i^b(r) = \mathbf{\Phi}^b(\mathbf{r})\mathbf{p}^b. \tag{4}$$

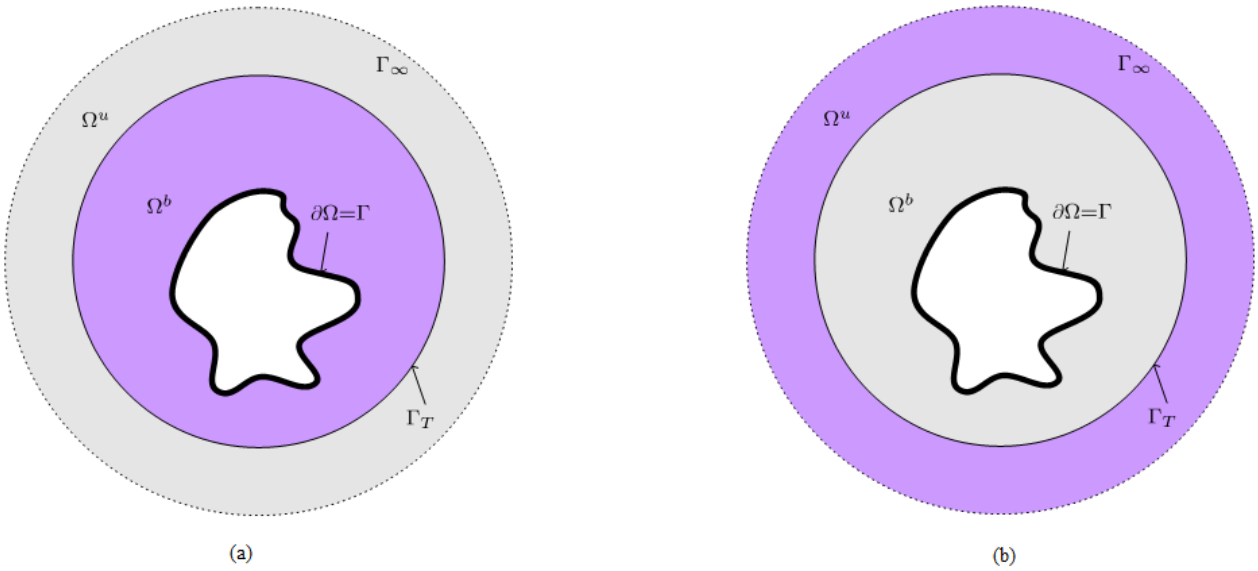

Figure 2: (a) bounded acoustic radiation domain, (b) unbounded acoustic radiation domain

For the 3D bounded domain three sets of wave functions $\mathbf{\Phi}^b(\mathbf{r})$ are distinguished and referred to as *r*- , *s*- and *t*- sets

$$\mathbf{\Phi}^b(\mathbf{r}) = \begin{cases} \Phi_r(x,y,z) = \cos(k_{rx}x)\cos(k_{ry}y)e^{-jk_{rz}z} \\ \Phi_s(x,y,z) = \cos(k_{sx}x)e^{-jk_{sy}y}\cos(k_{sz}z) \\ \Phi_t(x,y,z) = e^{-jk_{tx}x}\cos(k_{ty}y)\cos(k_{tz}z) \end{cases}. \tag{5}$$

Each function in the *r*-, *s*- and *t*-sets is an exact solution of Helmholtz equation (1), as long as the wave numbers in (5) satisfy

$$k_{rx}^2 + k_{ry}^2 + k_{rz}^2 = k_{sx}^2 + k_{sy}^2 + k_{sz}^2 = k_{tx}^2 + k_{ty}^2 + k_{tz}^2 = k^2. \tag{6}$$

As a result, an infinite number of wave functions (5) can be defined for the expansion (4). The wave number components are selected as follows [1]

$$k_r = \begin{cases} k_{rx} = \dfrac{r\pi}{L_x}, & r = 0,1,2,...n_r \\ k_{ry} = \dfrac{r\pi}{L_y} \\ k_{rz} = \pm\sqrt{k^2 - k_{rx}^2 - k_{ry}^2} \end{cases} \tag{7}$$

$$k_s = \begin{cases} k_{sx} = \dfrac{s\pi}{L_x}, & s = 0,1,2,...n_s \\ k_{sy} = \pm\sqrt{k^2 - k_{sx}^2 - k_{sz}^2} \\ k_{sz} = \dfrac{s\pi}{L_z} \end{cases} \tag{8}$$

$$k_t = \begin{cases} k_{tx} = \pm\sqrt{k^2 - k_{ty}^2 - k_{tz}^2} \\ k_{ty} = \dfrac{t\pi}{L_y}, \qquad t = 0, 1, 2, ...n_t. \\ k_{tz} = \dfrac{t\pi}{L_z} \end{cases} \tag{9}$$

The integer sets *r*, *s* and *t* determine the degrees of freedom of the interior model and L_x, L_y and L_z are the dimensions of the smallest rectangular domain enclosing the considered problem acoustic subdomain.

3.2 Unbounded domain

The wave functions for the unbounded domain are chosen to implicitly obey the Sommerfeld radiation condition (3):

$$p(r, \vartheta, \varphi) \approx \sum_{l=0}^{L} \sum_{m=-l}^{l} p_{lm}^u h_l^{(2)}(kr) Y_l^m(\vartheta, \varphi) \tag{10}$$

with *r*, ϑ and φ the radial, azimuthal and zenithal spherical coordinates. In solution expansion (10) $h_l^{(2)}(kr)$ is the spherical Hankel function of the second kind, which representing the radial decay function

$$h_l^2(kr) = \sqrt{\frac{\pi}{2kr}} H_{l+\frac{1}{2}}^2(kr). \tag{11}$$

Y_l^m are the spherical harmonics [7], which correspond to the angular portion of the differential equation solution

$$Y_l^m(\vartheta, \varphi) = \sqrt{\frac{2l + 1(l-m)!}{4\pi(l+m)!}} P_l^m(cos\vartheta) e^{im\varphi}. \tag{12}$$

Expansion (10) may be rewritten in an analogous way as the pressure approximation in the bounded part of the wave model (4)

$$p^u(r) \approx \hat{p}^u(r) = \sum_{l=0}^{L} \sum_{m=-l}^{l} p_{lm}^u \Phi_i^u(r) = \mathbf{\Phi}^u(\mathbf{r}) \mathbf{p}^u \tag{13}$$

with $\mathbf{\Phi}^u(\mathbf{r})$ the wave function set

$$\mathbf{\Phi}^u(\mathbf{r}) = \mathbf{\Phi}^u(r, \vartheta, \varphi) = h_l^{(2)}(kr) Y_l^m(\vartheta, \varphi). \tag{14}$$

3.3 Acoustic wave model

The proposed function expansions (5) and (14) guarantee compliance with the Helmholtz equation inside the domain and the Sommerfeld radiation condition at infinity. The boundary conditions and subdomain continuity are enforced through a weighted residual formulation. The residuals on the boundary conditions are given in (2a), (2b) and (2c). For each subdomain, the error functions are orthogonalized with respect to a weighting function ***p(r)*** or its derivative. Like in the Galerkin weighting procedure, used in the FEM,

the weighting functions *p(**r**)* are expanded in the same set of acoustic wave function used in the pressure expansion (4) and (13).

Since the weighted residual formulation should hold for any weighting functions *p(r)*. This yields to a set of linear equation in the n_w unknowns wave function contribution factors which can be presented as:

$$[A]\{P_w\} = \{F\}. \tag{15}$$

As for the BEM and in contrast with the FEM, the proposed technique yields a fully populated matrix, whose elements are complex and which cannot be decomposed into frequency independent submatrices. The big advantage of the WBT is, however, that the system matrices are substantially smaller in comparison with the element based techniques.

4 Virtual Boundary Concept (VBC)

The WBT has shown to be efficient in modeling of 3D acoustic radiation problems. However, when a complex boundary shape is to be handled, the ability of the standard WBT is limited. When applying the WBT, the used global shape functions require convex or geometrically restricted fluid subdomains. In most practical applications polygonal domains, or domains with simple curvatures are handled, to simplify the surface parametrization and the efforts of the numerical integration. On the other hand, by refining the domain subdivision, the wave based model boundary can be more likely to the original problem boundary, but the efficiency of WBT starts to degrade, as the number of subdomains excessively increases.

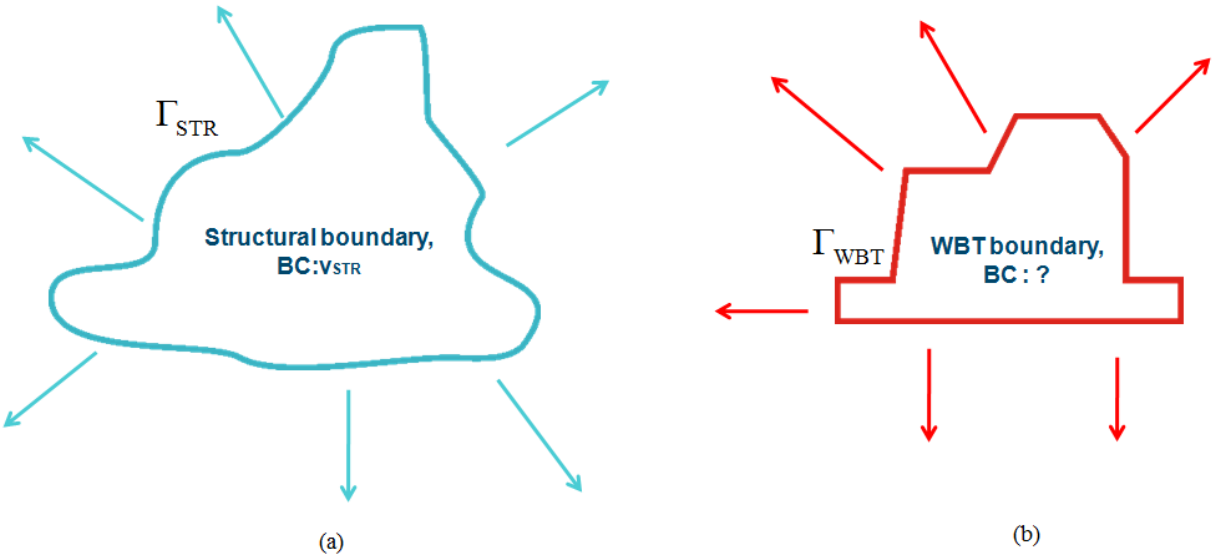

Figure 3: (a) acoustic radiation of structure, (b) acoustic radiation of wave based surfaces

The mentioned facts usually lead to a geometrical simplification of the model boundary (ie. as depicted on figure 3) and the application of a mapping procedure, where the boundary data of the original complex boundary shape Γ_{STR} (ie. nodal velocities of an FE mesh) is mapped (inter-, and extrapolated) onto the wave based model boundaries Γ_{WBT}.

A standard technique to map nodal velocities from the complex structural boundary Γ_{STR} to the wave based boundary Γ_{WBT} is the Inverse Distance Weighted interpolation (IDW), where the nodal data is extra/interpolated onto the integration quadrature points of Γ_{WBT} in the following way:

$$v(\mathbf{r}_i) = \sum_{j=1}^{N} \frac{\beta}{d_j} v_j^{FEM} \tag{16}$$

where $v(\mathbf{r}_i)$ is a quadrature point on Γ_{WBT}, v_j^{FEM} are the nodal velocities on Γ_{STR}, $d_j = \|\mathbf{r}_i - \mathbf{r}_j\|_2$ the distance between the quadrature point and the given FE node and β is a scaling factor, so that $\sum_{j=1}^{N} \frac{\beta}{d_j} = 1$.

Such a geometrical mapping does not consider the effect of the geometrical deviation or physical gap between the wave based model boundaries Γ_{WBT} and the original boundary shape Γ_{STR}.

In order to minimize the approximation error caused by the gap between a complex boundary Γ_{STR} and the wave based boundary Γ_{WBT}, a Virtual Boundary Concept (VBC) is introduced. The main idea of the VBC is an inverse approach to reconstruct the original boundary data on Γ_{STR} (ie. normal velocity) by a combination of WBT solutions, which finally result in an approximation of the original radiation problem (figure 3). This inverse problem poses the following two tasks:

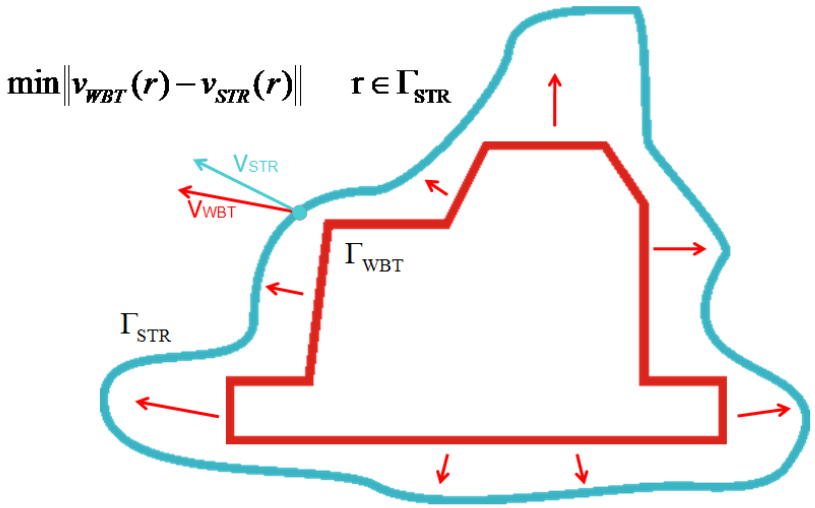

Figure 4: Virtual Boundary Concept (VBC)

- find an appropriate set of boundary conditions for the WBT model, whose set of solution can describe the original boundary data efficiently and accurately.
- find the optimal linear combination of these set of solutions to minimize approximation error on the complex boundary Γ_{STR} (from now on, virtual boundary).

In order to accomplish these two tasks, the complex boundary should be located strictly outside of the WB boundary (figure 4), resulting in the substitution of the original radiating boundary (virtual boundary) by the WB model.

4.1 Formulation of the Virtual Boundary Concept

The VBC can be formulated as the following sequence: In order to have a set of *n*- wave based solutions, a set of velocity boundary conditions v_{w_i} over the wave based surface are assigned

$$W = [v_{w_1}, v_{w_3}, v_{w_3}, ..., v_{w_n}], \tag{17}$$

One of the characteristics of the wave based model (15) is, that in case of velocity boundary type Γ_v the system matrix [A] is invariant with changing the boundary values as long as the geometrical shape of the boundary is still the same. This can be interpreted mathematically as in equation

$$[A][p_{w_1}, p_{w_2}, ..., p_{w_n}] = [f_1, f_2, ..., f_n], \tag{18}$$

where $[f_1 : f_n]$ are the right hand sides corresponding to each pre-assigned velocity shape and $[p_{w_1} : p_{w_n}]$ are WBT solution vectors resulting from the multiple right hand sides. For each WBT solution vector $[p_w]$, a normal velocity at the virtual boundary can be obtained

$$v_{post_i} = \frac{j}{\rho\omega}\left(\left[\frac{\partial\Phi_i}{\partial\bar{n}}\right]p_{w_i}\right). \tag{19}$$

A linear combination of the post processed velocities can be constructed

$$v_{approx} = \sum_{i=1}^{n} a_i v_{post_i} = \frac{j}{\rho\omega}\sum_{i=1}^{n} a_i\left(\left[\frac{\partial\Phi_i}{\partial\bar{n}}\right]p_{w_i}\right), \tag{20}$$

where $\bar{n}$ is the local normal vector. The weighting factors a_i of equation (20) are supposed to minimize error between the reconstructed velocity v_{approx} and the structural normal velocity v_{str}

$$\|e\| = \|v_{approx} - v_{str}\| \rightarrow min. \tag{21}$$

From above it is clear, that there are two tasks should be addresses regarding VBC

- find an appropriate set of pre-assigned velocities shapes for the WBT model, whose set of solutions can describe the original boundary data efficiently and accurately.
- the minimizing technique of the objective function (21).

These will be addressed in the following sections.

4.2 Pre-assigned velocities shapes

The choice of pre-assigned velocities shapes should be based on two main factors, physically reasonable set of velocities which can describe the structural velocities. Furthermore, the application of these velocity sets should not require relevant, additional computational efforts.

For the above reasons each planar surface of the WB boundary Γ_{WBT} inside the virtual boundary Γ_{STR} is treated as thin plates.

The steady-state out-of-plane displacement w_z can be approximated by a set of wave functions [9]. The wave functions (5) are used to describe the out of plane displacement and consequently normal velocity for each plate of the WB boundary surfaces.

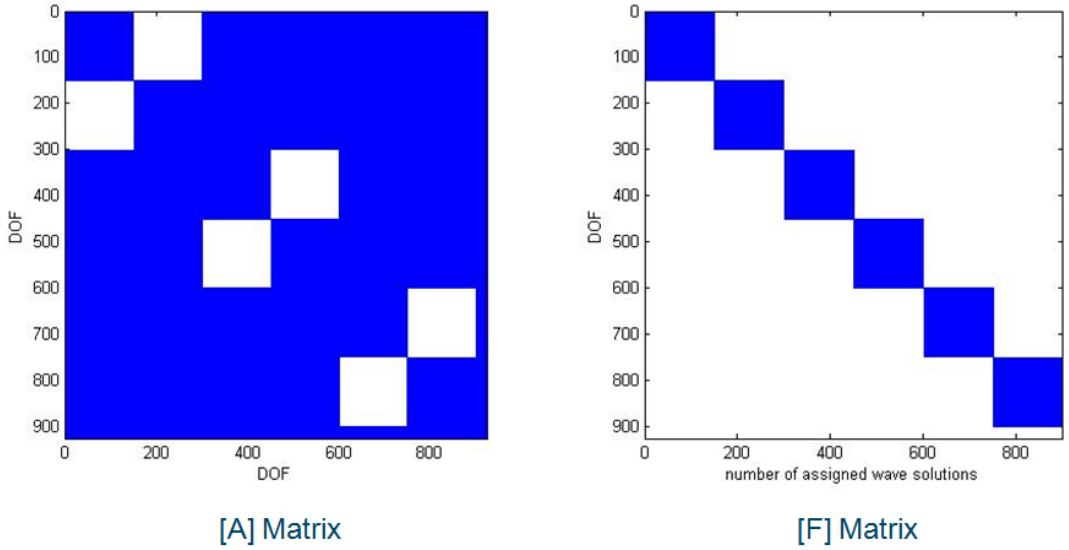

Figure 5: System matrix for wave shapes boundaries

From above it can be shown, that using wave functions as pre-assigned velocities over the WB boundary surfaces can verify both physical requirements and modeling simplicity.

By use of the wave functions as set of pre-assigned velocities over the wave based surfaces the system matrices for WBT subdomain (18) are as shown in figure 5.

4.3 Optimization technique

The optimization problem (21) is formulated as least squares problem.

Matrix Y represents an assembly of the resulted field velocities on the virtual boundary Γ_{STR} for each velocity boundary condition, practically for the individual columns of matrix F

$$Y = [v_{post_1}, v_{post_2}, v_{post_3}, ..., v_{post_n}]\,. \tag{22}$$

Equation (20) can be reformulated in matrix form as:

$$v_{approx} = Y\{a\} \tag{23}$$

with $\{a\}$ is column vector of *n* linear weighting factors. The error between the reconstructed velocity and the structural normal velocity v_{str} is defined in the second Euclidean norm as:

$$\|e\|_2^2 = \|Y\{a\} - v_{str}\|_2^2 \rightarrow min, \tag{24}$$

which leads to

$$\nabla \|Y\{a\} - v_{str}\|_2^2 = 2Y^H Y\{a\} - 2Y^H v_{str} = 0 \tag{25}$$

and finally resulting in the linear equation system

$$Y^H Y\{a\} = Y^H v_{str} \tag{26}$$

for the coefficient vector $\{a\}$.

Although $Y^H Y$ is ill conditioned the standard pre-conditioned conjugate gradient was found to be efficient to solve equation (26).

5 Application example

In order to validate the VBC for complex boundary shapes, the curved boundary shape depicted on figure 6b was considered. The WB model is defined inside this shape to satisfy the necessary condition of VBC (figure 6a and 6c). The curved boundary itself was modelled as a shell FEM mesh, excited by a point force $F = 1\,N$ z- axis direction (figure 6b).

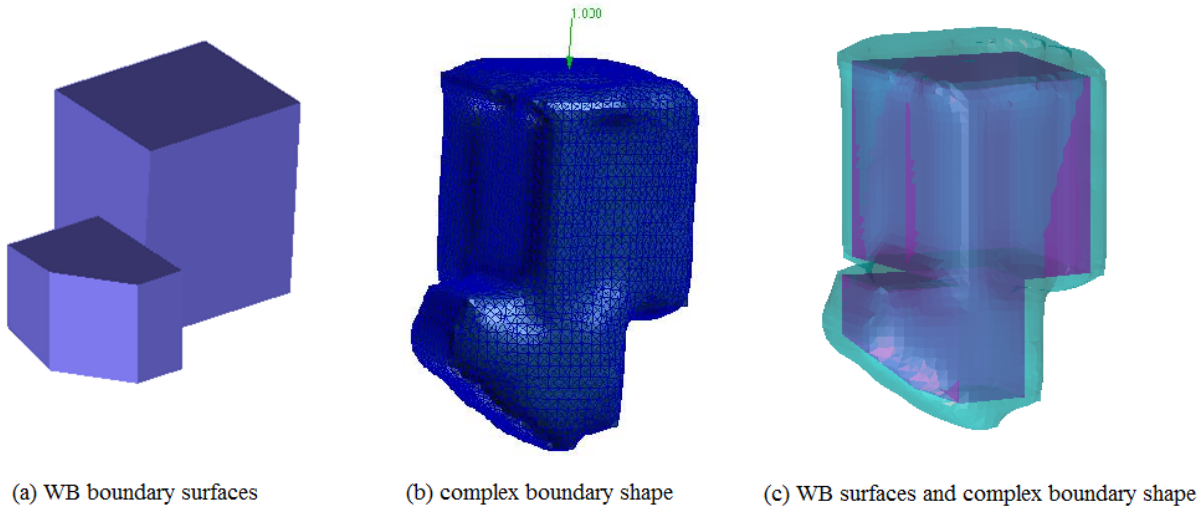

(a) WB boundary surfaces (b) complex boundary shape (c) WB surfaces and complex boundary shape

Figure 6: Engine model arrangement

The FE mesh is an aluminium shell with thickness *t= 3 mm*, density $\rho_s = 2700\,kg/m^3$, Young's modulus $E = 72.10^9\,N/m^2$ and the Poisson's ratio $\nu = 0.3$. The FE model is solved by MSC. NASTRAN structural dynamics harmonic frequency response solver. The structural velocity results are considered as reference results for the error minimization (25).

The model is surrounded by air with density $\rho = 1.9985\,kg/m^3$ and speed of sound $c = 343.799\,m/s$. The acoustic radiation calculations were carried out by using a BEM reference model. The BE mesh was equivalent with the FE structural mesh and was solved by LMS sysnoise 5.6 direct exterior collocation solver.

The BEM reference model and the evaluated field point mesh are shown on figure 7a. The WB boundary surfaces and field points mesh are shown in figure 7b. The structural normal velocity magnitude and reconstructed normal velocity using VBC are shown in figure 8.

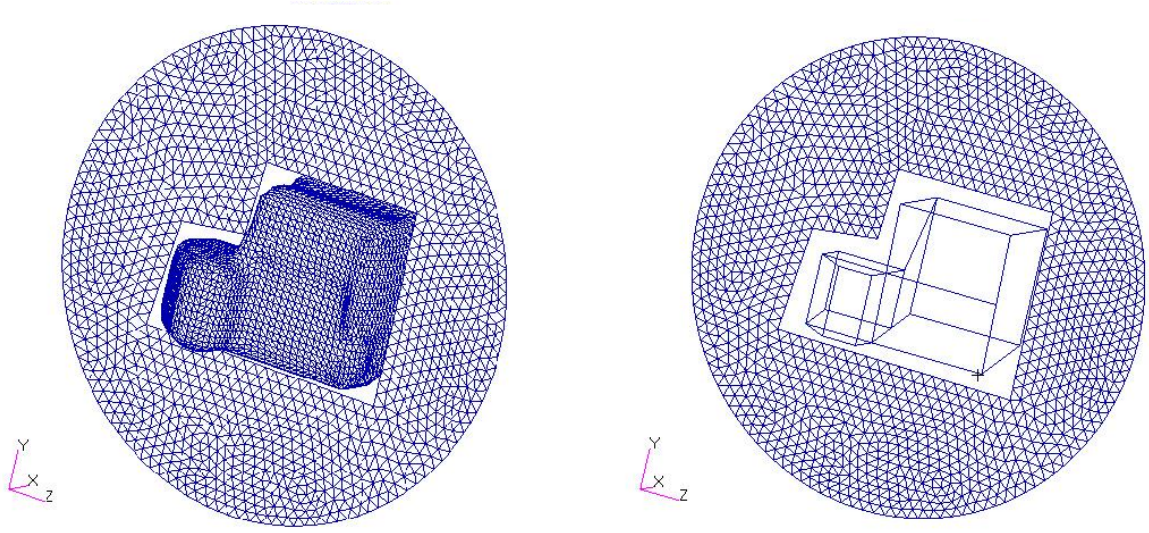

(a) BEM reference model (B) WBT model

Figure 7: BEM-WBT contour plan

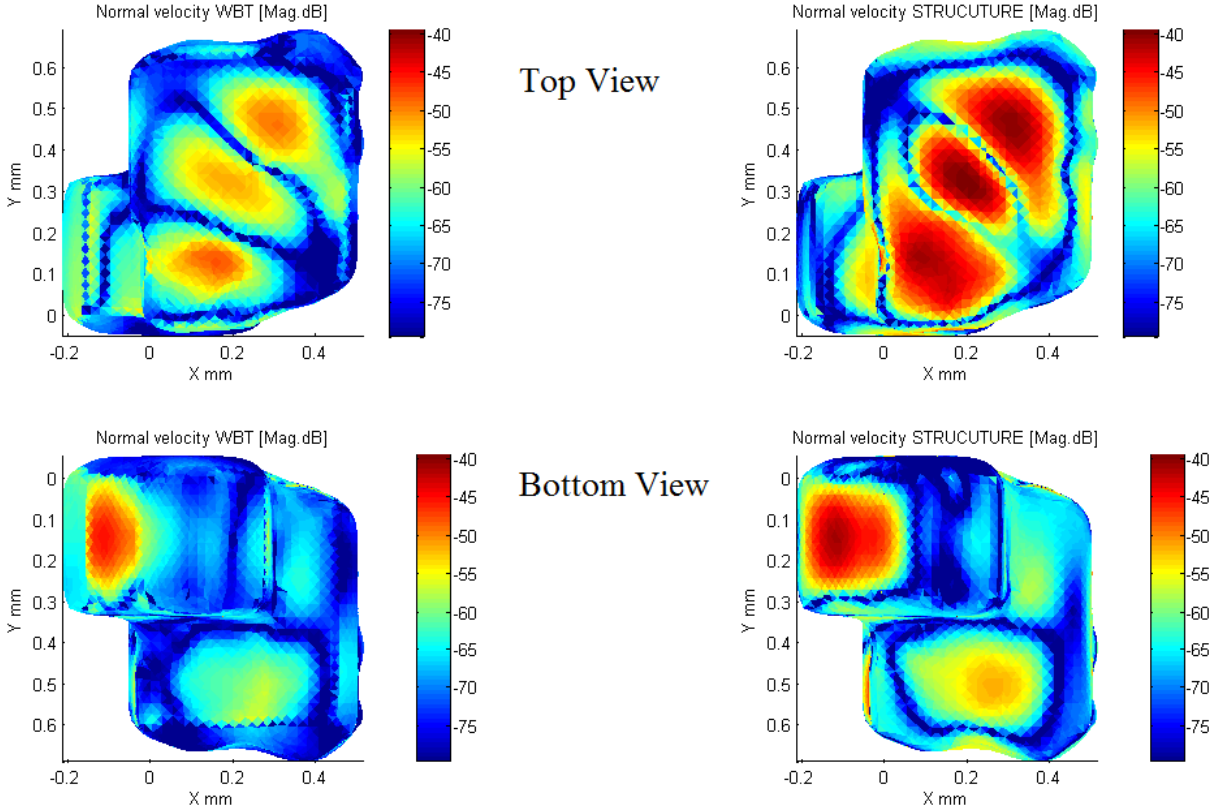

Figure 8: Normal velocity magnitude in dB constructed by VBC at 380 Hz (left), Normal structural velocity magnitude in dB at 380 Hz (right)

In order to evaluate the performance of VBC, the average relative error of normal velocity is calculated over the frequency range 100 to 1000 Hz with step 40 Hz. The average relative error is evaluated at the structural boundary with reference to the structural normal velocity for both VBC and mapping method (figure 9). Furthermore, to assess the efficiency of the VBC approach, a comparison was made between

results obtained by the VBC and the IDW mapping procedure (16).

As shown in figure 9, application of VBC has enhanced the average relative error of normal velocity in comparison with the error caused by mapping method.

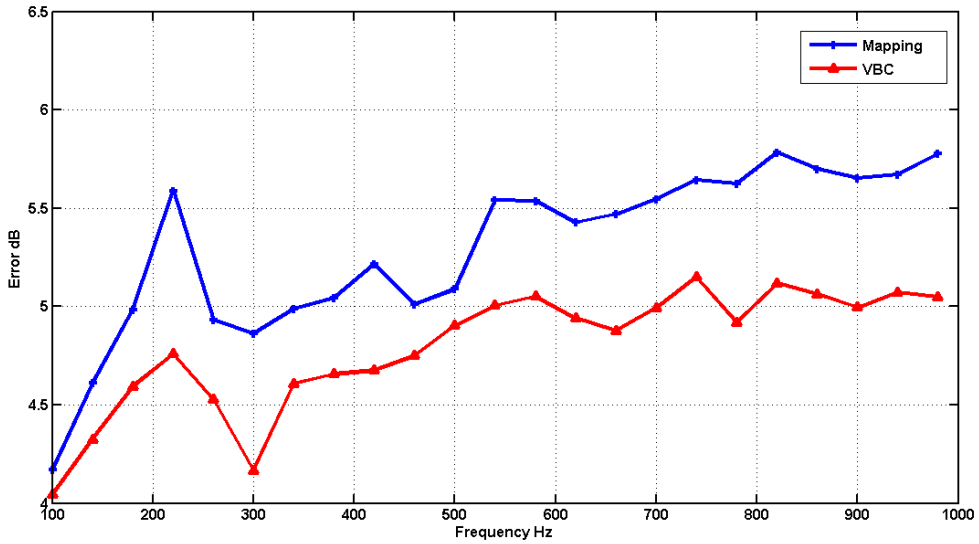

Figure 9: Average relative error of normal velocity in dB

The sound field pressure results are calculated at the field point mesh which are shown in figure 7. BEM results are used as reference in average error calculations. Figure 10 shows the sound field pressure in dB for both VBC and BEM results.

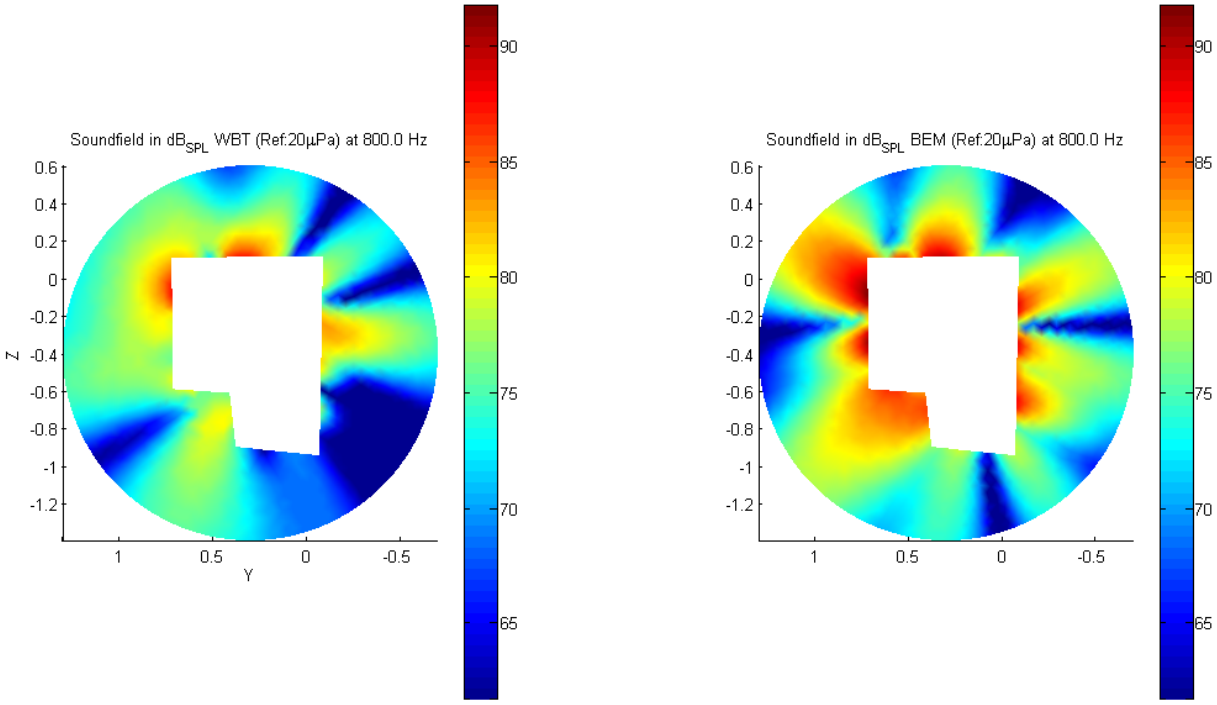

Figure 10: Sound field in dB_{SPL} VBC (left), Sound field in dB_{SPL} BEM (right)

The average relative error of acoustic pressure is calculated over the frequency range 100 to 1000 Hz with step 40 Hz. The average relative error is evaluated at field point mesh with reference to the BEM results for both VBC and mapping method (figure 11).

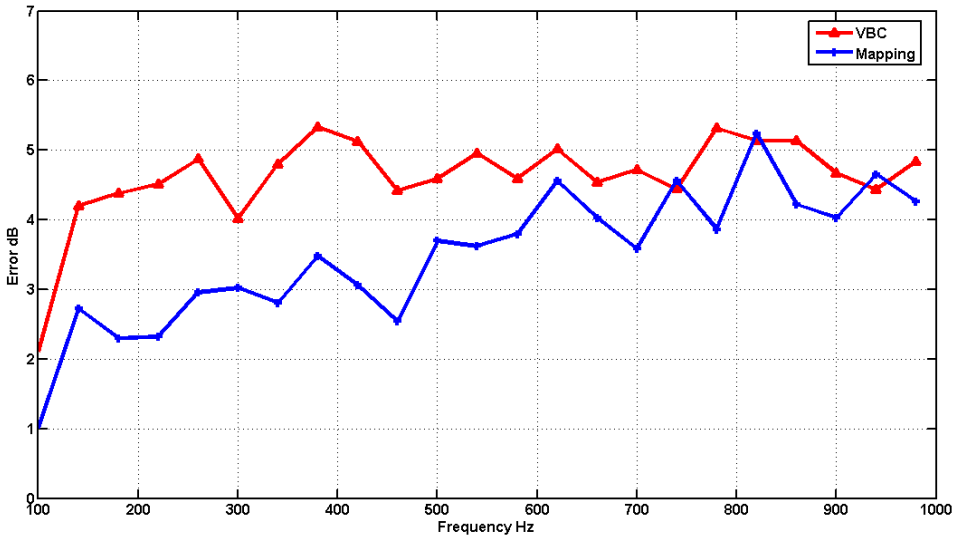

Figure 11: Average pressure relative error in dB

6 Conclusion and future work

This paper applies a novel approach of Virtual Boundary Concept (VBC) to aid WBT to handle complex boundary shapes. The main idea is to substitute the complex boundary shape, located outside the WB boundary surface, with a virtual boundary, whose velocity distribution is approximated by linear combinations of elementary WB solutions. It is illustrated through analysis for simplified engine model example, that the accuracy is enhanced compared to currently used mapping technique in the normal velocity results over the structure boundary. The accuracy of sound field pressure has shown some degradation in comparison to mapping technique.

From practical point of view VBC can compensate errors due to minimization problem in addition to the error generated by WBT solution without increasing of the system size.

Future research activities will focus on the enhancement of VBC results by advising some other alternatives of the pre-assigned velocities shapes, objective function and optimization technique.

Acknowledgments

The author gratefully acknowledge the ITN Marie Curie project GA-2008-214909 (MID-FREQUENCY - CAE Methodologies for Mid Frequency Analysis in Vibration and Acoustics). Furthermore, the authors would like to acknowledge the financial support of the COMET K2 Competence Centres for Excellent Technologies Programme of the Austrian Federal Ministry for Transport, Innovation and Technology (BMVIT), the Austrian Federal Ministry of Economy, Family and Youth (BMWFJ), the Austrian Research Promotion Agency (FFG), the Province of Styria and the Styrian Business Promotion Agency (SFG).

References

[1] W. Desmet, *Wave based prediction technique for coupled vibro-acoustic analysis, Ph.D. thesis 98D12*, Katholieke Universiteit Leuven, Leuven, Belgium (1998).

[2] B. Pluymers, *Wave based modeling methods for steady-state vibro-acoustics, Ph.D. thesis 06D4*, Katholieke Universiteit Leuven, Leuven, Belgium (2006).

[3] C. T. Kelley, *Iterative method for optimization- SIAM publications*, Society for industrial and applied mathematics, SIAM, Florida, USA (1999).

[4] E. Kita, N. Kamiya *Trefftz method: An overview*, Advanced in Engineering software 24 (1995) 3-12.

[5] T. Mocsai, H.-H. Priebsch, *Engine radiation simulation up to 3khz using the Wave Based Technique*, *Proceedings of The 2009 International Congress of sound and vibration ICSV 16*, Karakow, Poland, 2009.

[6] B. Bergen, B. Van Genechten, B. Pluymers, D. Vandepitte, W. Desmet, *An efficient multi-level wave based modeling concept for acoustic radiation and scattering problems*, *Proceedings of the International Conference on Noise and Vibration Engineering ISMA 2008*, Leuven, Belgium, pp. 133-146, 2008.

[7] J. Rejlek, B. Pluymers, A. Hepberger, H.-H. Priebsch, W. Desmet, *Application of the Wave Based Technique for steady-state semi-infinite sound radiation analysis*, *Proceedings of the LSAME 2008 Trefftz Symposium*, Leuven, Belgium, pp. 349-364, 2008.

[8] A. Hepberger, F. Diwoky, K. Jalics, H.-H. Priebsch, *Application of the Wave Based Technique for cavity considering forced excitation at boundaries and effects of absorption materials*, *Proceedings of the International Conference on Noise and Vibration Engineering ISMA 2004*, Leuven, Belgium, 2004.

[9] K. Vergote, C. Vanmaele, D. Vandepitte, W. Desmet, *On use of an efficient wave based method for steady state structural dynamic analysis*, *Proceedings of the International Conference on Noise and Vibration Engineering ISMA 2008*, Leuven, Belgium, pp. 433-460, 2008.